ACS Chemical Neuroscience

pubs.acs.org/chemneuro Research Article

Binding Mechanisms of Amyloid-like Peptides to Lipid Bilayers and Effects of Divalent Cations

Yanxing Yang, Sharareh Jalali, Bradley L. Nilsson, and Cristiano L. Dias*

Cite This: *ACS Chem. Neurosci.* 2021, 12, 2027−2035 Read Online

ACCESS | Metrics & More | Article Recommendations | Supporting Information

ABSTRACT: In several neurodegenerative diseases, cell toxicity can emerge from damage produced by amyloid aggregates to lipid membranes. The details accounting for this damage are poorly understood including how individual amyloid peptides interact with phospholipid membranes before aggregation. Here, we use all-atom molecular dynamics simulations to investigate the molecular mechanisms accounting for amyloid−membrane interactions and the role played by calcium ions in this interaction. Model peptides known to self-assemble into amyloid fibrils and bilayer made from zwitterionic and anionic lipids are used in this study. We find that both electrostatic and hydrophobic interactions contribute to peptide−bilayer binding. In particular, the attraction of peptides to lipid bilayers is dominated by electrostatic interactions between positive residues and negative phosphate moieties of lipid head groups. This attraction is stronger for anionic bilayers than for zwitterionic ones. Hydrophobicity drives the burial of nonpolar residues into the interior of the bilayer producing strong binding in our simulations. Moreover, we observe that the attraction of peptides to the bilayer is significantly reduced in the presence of calcium ions. This is due to the binding of calcium ions to negative phosphate moieties of lipid head groups, which leaves phospholipid bilayers with a net positive charge. Strong binding of the peptide to the membrane occurs less frequently in the presence of calcium ions and involves the formation of a "Ca^{2+} bridge".

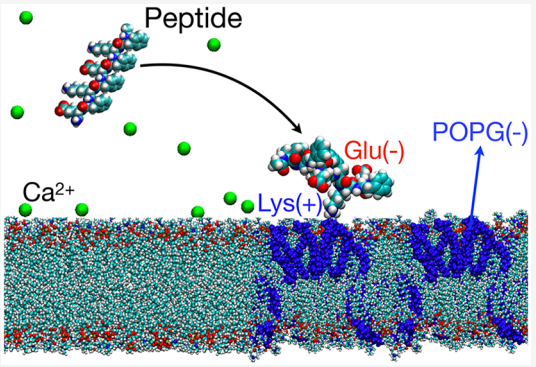

KEYWORDS: *Amyloid, lipid membrane, calcium, amyloid−membrane binding, calcium−membrane binding, Alzheimer's disease*

INTRODUCTION

Amyloid diseases, which include Alzheimer's and Parkinson's, are characterized by the aggregation of peptides into soluble oligomers and fibrils.[1−6] Interactions of these aggregates with the cell membrane accounts for an important mechanism of cell toxicity wherein annular shaped oligomers can form pores in lipid bilayers and amyloid fibrils can induce lipid loss through a detergent-like mechanism.[2,7−11] These types of damage increase the vulnerability of neurons, and they can lead to cell death.[12,13] Several factors have been shown to affect toxicity by amyloid peptides including lipid composition and the presence of ions in the solution.[14−27] Currently, the molecular mechanisms accounting for amyloid−membrane interactions remain poorly understood and further studies are needed to rationalize how these mechanisms are affected by lipid composition, ions, and pH. This fundamental knowledge is critical to better understand cell toxicity, and it may enable rational design of new therapeutics to treat amyloid diseases.

Insights into amyloid toxicity are often obtained experimentally by studying peptide aggregation in the presence of vesicles, monolayers, or supported/suspended lipid membranes.[22,23,28−30] Specifically, vesicles can contribute to either increase or decrease the rate of aggregation.[15,28,31−34] Decreased rates of aggregation have been related to the sequestration of peptides into the interior of the bilayer where, surrounded by lipids, it is more difficult for peptides to attract each other.[35] In some cases, increased rates of aggregation have been related to the ability of some lipids to attract and align peptides at the membrane surface facilitating the formation of amyloid fibrils.[14,15] Accordingly, anionic vesicles have been shown to induce peptide ordering at the bilayer surface and to increase the rate of amyloid fibril formation.[15,36] These results have been reproduced for different types of anionic lipids as well as peptide sequences highlighting the importance of electrostatic interactions in amyloid−bilayer binding. At first sight, it might appear counterintuitive that the rate of aggregation of negatively charged peptides, for example, the amyloid-β (Aβ) protein, increases in the presence of anionic membranes. However, Aβ has several positive residues distributed along its amino acid sequence, which can be attracted to the bilayer while keeping negative residues at a

Received: March 10, 2021
Accepted: April 26, 2021
Published: May 11, 2021

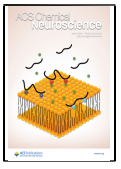

certain distance from it.[29,37] This counterintuitive behavior of Aβ was highlighted by Moores et al.[30] wherein this peptide was shown to bind positively and negatively charged, as well as nonpolar, surfaces because of its complex distribution of charged and nonpolar residues. In the same vein, binding of α-synuclein to membrane was shown to be driven by electrostatic interactions between positive lysine residues and lipid head groups.[38]

The importance of electrostatic interactions is further highlighted by the role played by calcium ions in amyloid aggregation at the surface of lipid membranes. Experimental studies consistently report that the addition of Ca^{2+} ions to solutions containing anionic bilayers promotes the aggregation of amyloid peptides independently of their net charge.[10,19,39] This has been related to a reduction in the peptide−membrane binding affinity and calcium's ability to promote the stability of lipid membranes, which may inhibit the sequestration of peptides into the bilayer.[10,19,39,40] Calcium's roles in regulating the formation of lipid domains and recruitment of ionic lipids to the membrane surface have also been proposed as mechanisms to explain its effect in aggregation.[41−43] In contrast to these results, an increase in the peptide−membrane binding affinity has also been reported for the Aβ peptide via the formation of "Ca^{2+} bridges" between negatively charged glutamic acid (E) residues and negatively charged phosphate moieties of lipid head groups.[20,44,45] The effect of calcium in promoting aggregation close to anionic membrane has, however, been observed even for peptides that do not have negative residues, for example, amylin. This suggests mechanisms of action that do not depend on the presence of negative residues in the peptide sequence.

Computational studies have been providing important insights into the mechanism of amyloid−membrane binding.[21,46−50] Recent studies have shown that the nonpolar segments of amyloid peptides, for example, the C-terminal residues and the central hydrophobic core of Aβ, are the first to be inserted into the bilayer interior.[51] This highlights the importance of hydrophobic interactions. In these simulations, amyloid peptides cause the bilayer to become thinner and the area per lipid to reduce significantly wherein the fatty acid tail of lipids become strongly disordered.[46,51,52] Despite these important insights, most simulations have not been designed to study the attraction of amyloids to lipid membranes as they are performed with peptides already deposited on the bilayer surface. For the latter study, a large fraction of the simulation box needs to be dedicated to the solvent, which is computationally expensive but necessary to understand how peptides in solution approach the membrane.

Here, we use molecular dynamics simulations to provide atomic insights into the interactions accounting for the attraction and binding of individual amyloid-like peptides, i.e., monomers, to lipid bilayers and the effect of calcium ions in this process. As shown in Figure 1, a large fraction of the simulation box is dedicated to the solvent in our simulations. We show that the attraction of peptides to membranes is dominated by electrostatic interactions between *positively* charged residues and *negatively* charged phosphate groups of lipids. Moreover, when the peptide is at close proximity to the membrane, hydrophobicity drives the burial of nonpolar residues into the bilayer, which produces strong binding in our simulations. These modes of interaction were observed for both zwitterionic and anionic bilayers wherein the attraction of positive residues is more pronounced in the latter membrane.

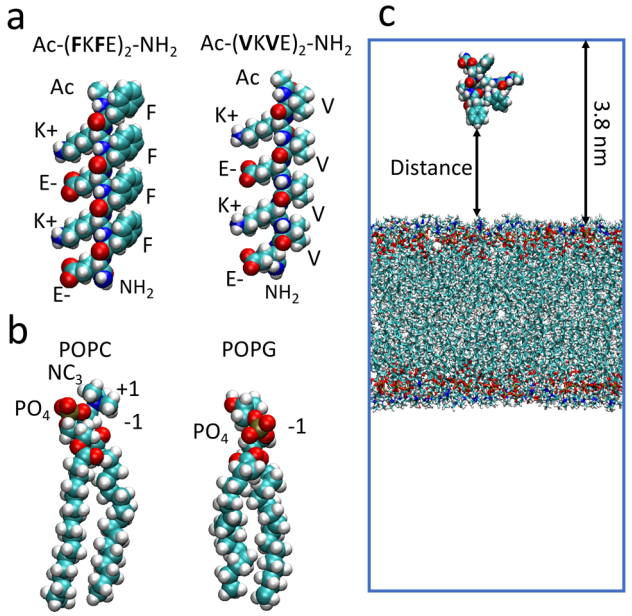

Figure 1. Atomic representation of (a) peptides and (b) lipids studied in the work. Cyan, white, blue, red, and orange represent carbon, hydrogen, nitrogen, oxygen, and phosphate atoms, respectively. (c) Schematic representation of the simulation box and the minimum distance between peptide and lipid bilayer.

We also show that Ca^{2+} ions bind strongly to phosphate groups of the lipid bilayer[53,54] shielding electrostatic interactions between positively charged residues and the membrane. This accounts for a significantly weaker attraction of peptides to membranes in our simulations. Strong binding of peptides to lipid membranes occurs less frequently in the presence of calcium ions, and it involves the formation of Ca^{2+} bridges between negatively charged E residues and negatively charged phosphate moieties of lipids.

RESULTS AND DISCUSSION

Zwitterionic Bilayer. A schematic representation of the simulation box and the shortest distance ξ between lipid and peptide atoms is shown in Figure 1c. The time dependence of ξ is depicted in Figure 2a,b for two trajectories simulated using the F-sequence and the PC bilayer in the absence of $CaCl_2$. In panel a, the peptide undergoes several binding−unbinding events, and in panel b it binds strongly to the membrane after an induction time of 200 ns. A characteristic configuration of the peptide in this strong binding state is shown in the inset of panel b wherein nonpolar phenylalanine side chains are buried within the dry core of the bilayer and charged side chains are facing the solvent interface. In three out of the five 600 ns simulations performed for this system, the peptide binds strongly to the bilayer after 200, 250, and 500 ns, see section S2. For the less hydrophobic V-sequence, the peptide binds strongly to the bilayer after 200 ns in only one of the five simulations, see section S2. In the presence of Ca^{2+} ions, the F-peptide did not bind strongly to the bilayer in any of the five simulations, see section S2. This is an indication that anchorage of peptides to the bilayer can be reduced by decreasing the hydrophobic character of the sequence and by adding ions to the solution.

To quantify peptide−bilayer interactions, all the simulations are identified as two regions referred to as induction time and strong binding. All the analysis in this work is run on these two

https://doi.org/10.1021/acschemneuro.1c00140
ACS Chem. Neurosci. 2021, 12, 2027−2035

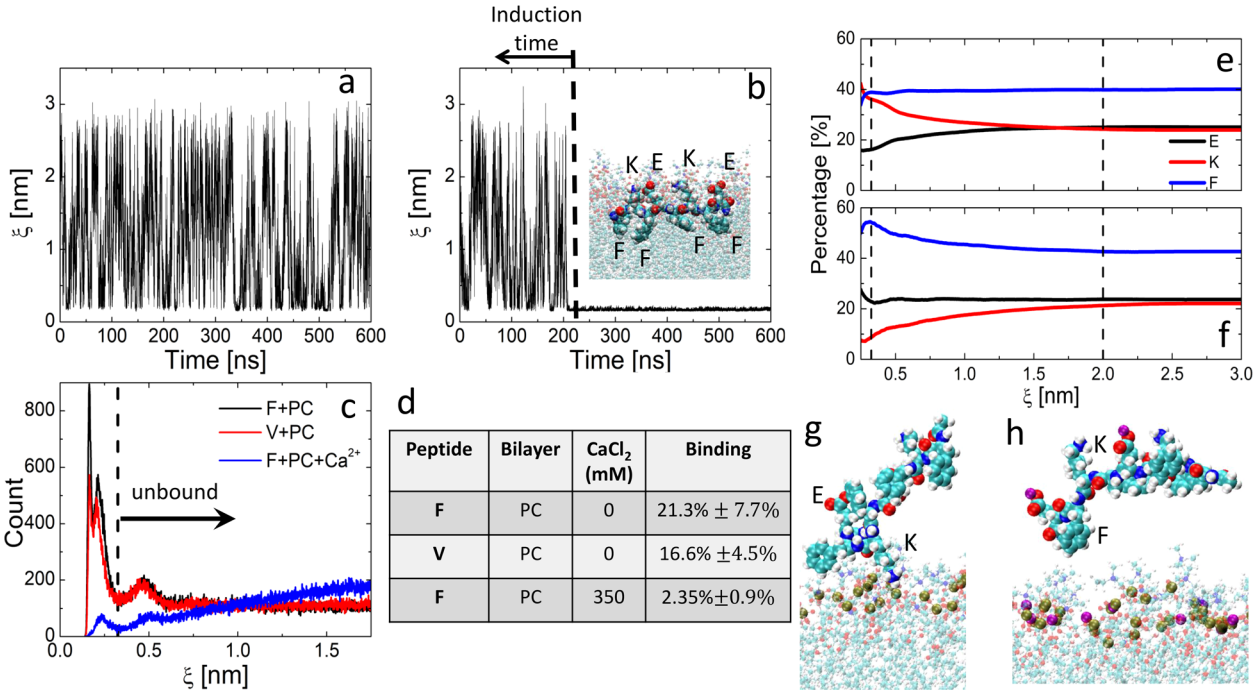

Peptide	Bilayer	$CaCl_2$ (mM)	Binding
F	PC	0	21.3% ± 7.7%
V	PC	0	16.6% ±4.5%
F	PC	350	2.35%±0.9%

Figure 2. Peptide binding to zwitterionic (PC) bilayers. Time dependence of peptide−bilayer distance for simulations performed using F-peptide (a) without and (b) with strong binding. Inset of panel b shows a configuration in which the peptide is bound strongly to the bilayer with F side chains buried within the lipid tail. (c) Distance distribution computed during the induction time of simulations performed using F- and V-peptides in the absence and presence of 350 mM $CaCl_2$. (d) Percentage of time F- and V-peptides are bound to the bilayer in the absence and presence of 350 mM $CaCl_2$. Percentage of bound states at a distance ξ for which E, K, or F residues are closer to the membrane in the (e) absence and (f) presence of $CaCl_2$. Characteristic configurations showing (g) a lysine side chain being attracted to phosphate atoms (in beige) in the absence of $CaCl_2$ and (h) calcium ions (in purple) being attracted to phosphate atom and repelling lysine side chains.

regions separately and takes all the replicas into account. Figure 2c depicts histograms of ξ computed during the induction time of our simulations. These histograms exhibit three main peaks with maxima at 0.17, 0.21, and 0.47 nm. The first two peaks are characterized by configurations in which atoms of several residues are in direct contact with lipids in the bilayer whereas the peptide remains mainly solvated in the third peak. Thus, the minimum between second and third peaks, i.e., ξ_{cutoff} = 0.325 nm, can used as a cutoff to discriminate between membrane bound and unbound states of the peptide. Histograms of simulations performed using F- and V-sequences in the absence of ions differ mainly in the first two peaks, which are less pronounced for the less hydrophobic V-peptide. When $CaCl_2$ is added to the solution, the first two peaks of the F-sequence become significantly less pronounced and the probability of finding the peptide at ξ increases with increasing ξ. This suggests that $CaCl_2$ renders the zwitterionic bilayer repulsive to the peptide. The table in Figure 2d summarizes these results by showing the percentage of peptide−bilayer binding events of our simulations. This percentage is computed from the histogram in Figure 2c using ξ_{cutoff}. Reducing the hydrophobic character of the peptide decreases the percentage of binding events in the simulation from 21% for phenylalanine to 16% for valine. Adding $CaCl_2$ to the solution has an even stronger effect as it reduces the population of binding events to 2%.

Figure 2e−f provides insights into the chemical groups that are attracted to the bilayer by tracking the type of residues that are closest to the membrane at a distance ξ. For large peptide−bilayer distances (i.e., $\xi \geq 2$ nm), 40% of all configurations in our trajectories have nonpolar residues (i.e., F) closer to the membrane. Configurations in which positive (K) and negative (E) residues are closer to the bilayer account for 25% and 25%, respectively, of all frames. The remaining 10% of frames (not shown in the figure) correspond to configurations in which the N-terminal (acetyl group) is the closest chemical group to the bilayer. These numbers are mostly consistent with the percentage of F (i.e., 44%), E (22%), and K (22%) amino acids in the peptide sequence, and they reflect a situation in which the peptide is not interacting with the bilayer.

In the absence of $CaCl_2$ (see Figure 2e) and as ξ decreases, the percentage of K-configurations, that is, configuration in which K is the closest residue to the membrane, increases significantly from 25% to 35%, see red line. Concurrently, E-configurations (black line) become proportionally less populated whereas the percentage of F-configurations (blue line) is mostly unaffected by the minimal peptide−bilayer distance. This highlights the importance of electrostatics in peptide−bilayer interactions wherein positively and negatively charged amino acids are attracted to and repelled from the bilayer, respectively. A characteristic configuration illustrating this type of peptide−bilayer interaction is shown in Figure 2g wherein a positively charged K residue is attracted to negatively charged phosphate atoms of POPC (large beige spheres), which repel negatively charged E residues.

In the presence of $CaCl_2$ (Figure 2f) and as ξ decreases, the percentage of K-configurations decreases from 22% to 9%, whereas the number of E-configurations remain mostly insensitive to the peptide−bilayer distance. Concurrently, the percentage of F-configurations increases from 40% to 55%. A characteristic configuration wherein F residues are close to the bilayer is shown in Figure 2h. This figure also depicts Ca^{2+} ions

https://doi.org/10.1021/acschemneuro.1c00140
ACS Chem. Neurosci. 2021, 12, 2027−2035

(purple spheres), which are attracted to negatively charged phosphate atoms (beige) of POPC lipids. We find that on average every fourth POPC lipid becomes bonded to one Ca^{2+} ion consistent with other studies,[53,54] see also Figure S2. This renders the bilayer positively charged leading it to repel K residues and accounting for fewer K-configurations in the trajectory. To explain the increased percentage of F-configuration with decreasing ξ in panel f requires noticing that nonpolar and charged residues face opposite sides of our amphipathic peptides (see Figure 1a). Thus, repulsion of K residues leaves the nonpolar side of the peptide facing the bilayer, which accounts for the increased percentage of F-configurations with decreasing ξ.

Recent studies have suggested that the binding strength of Ca^{2+} to lipid bilayers may be overestimated in most force fields.[54] Accordingly, corrections to the Ca^{2+} force field have been proposed including the electronic continuum correction with rescaling (ECCR)[55] and the pair-specific nonbound fixed optimized Lennard-Jones parameters (NBFIX).[56] Since binding of calcium to the bilayer is critical to explain effects of this ion on peptide−membrane interactions, we also performed simulations with the NBFIX force field. In the Supporting Information, we show that the percentage of peptide−bilayer bound states in the presence of Ca^{2+} ions modeled with the NBFIX force field is 11% ± 1.7%, see section S3. Thus, the effect of $CaCl_2$ in discouraging binding of peptides to the bilayer is robust in simulations although its magnitude may depend on force field.

Figure 3a shows that the effect of the positively charged amino moiety of POPC lipids plays a lesser role in attracting peptides to the bilayer as it is exposed to the solvent and, thus, screened by it. In this figure, the average cosine of the angle between the dipole moment of water and the z-axis is plotted as a function of the z-coordinate of water. At distances larger than 1 nm, which corresponds to approximately three layers of water molecules, the average cosine is zero as water molecules do not have a preferential direction. Close to the bilayer, the net orientation of water molecules is consistent with their role in screening positive charges on the bilayer, that is, the average dipole moment points toward the membrane surface, as shown by red arrows in the inset of Figure 3a. Thus, interactions close to the bilayer interface are dominated by electrostatic interactions between the negatively charged phosphate moiety of POPC lipids and charged species in the solution. This moiety attracts positively charged residues of the peptide as well as cations. This latter renders the membrane positively charged and leads to the repulsion of positive residues. In the absence of cations, the negatively charged phosphate group of POPC attracts positively charged residues.

Our simulations also show that, when at close proximity to the lipid surface, nonpolar residues can bury themselves into the dry core of the bilayer, see inset of Figure 1b. This accounts for strong peptide−bilayer binding, which leaves the peptide anchored onto the membrane surface. A sequence of events leading to hydrophobic burial is shown in Figure 3b−e. Initially, the peptide is attracted to the membrane surface via one of its lysine residues (panel b) followed by the insertion of a nonpolar residue into the lipid bilayer, panel c. The latter residue acts like an anchor keeping the peptide close to the surface for an extended period of time, panel d. This allows other nonpolar residues to embed themselves into the bilayer, panel e. Since residues that are more hydrophobic can penetrate the bilayer more easily, sequences with a higher

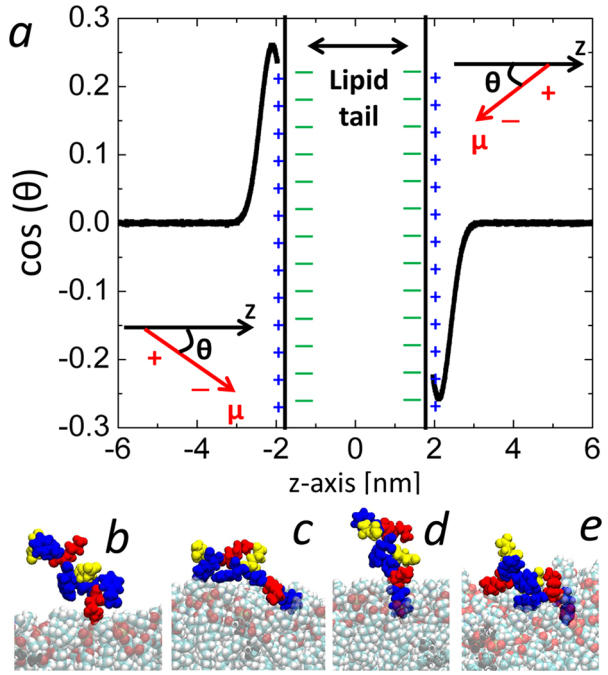

Figure 3. Screening of positive amino groups by water molecules and burial of nonpolar residues into the bilayer surface. (a) Average cosine of the angle θ between dipole moment μ of water and z-axis as a function of the z-coordinate of water molecules. The space occupied by lipid tails as well as positive (blue) and negative (green) moieties of head groups are shown schematically. The orientation of μ with respect to the bilayer surface is shown in red. (b−e) Burial of nonpolar residues (in blue) into the membrane. Red and yellow colors are used to represent lysine and glutamate amino acids. These figures correspond to simulations performed for the F-peptide in the absence of $CaCl_2$.

hydrophobic character are more prone to bind strongly to the bilayer as shown in Figure 2d.

Anionic Bilayer. To further highlight the role of electrostatic interactions in peptide−bilayer binding, we study the effects of anionic lipids in Figure 4. In panel a, percentages of binding events are shown for PC, PG_{10}, and PG_{30} bilayers in the absence (black symbols) and presence (red symbols) of $CaCl_2$. These quantities were computed from the induction time of the five simulations performed using the F-peptide. Replacing 10% of POPC lipids with anionic POPG does not account for a large change in the population of bound states. However, an increase of almost 10% in the population of bound states is observed when 30% of POPC lipids are replaced with POPG. Moreover, in four out of five trajectories, peptides bind strongly to PG_{30} bilayers before 100 ns. For zwitterionic PC bilayer (i.e., Figure 2), strong binding was observed in only three out of five trajectories after 250 ns. This highlights significantly stronger attraction and binding of peptides to anionic bilayers. To rationalize this effect of anionic lipids, Figure 4b,c shows the percentage of frames in which positive (K) and negative (E) residues are closer to the membrane than any other residues. For PG_{30} bilayers (dashed black lines), K and E residues are significantly closer to and further from the membrane, respectively, when compared to PC bilayers (full black lines). This is consistent with positively charged residues being more strongly attracted to negatively charged moieties of anionic than to zwitterionic lipids.

https://doi.org/10.1021/acschemneuro.1c00140
ACS Chem. Neurosci. 2021, 12, 2027−2035

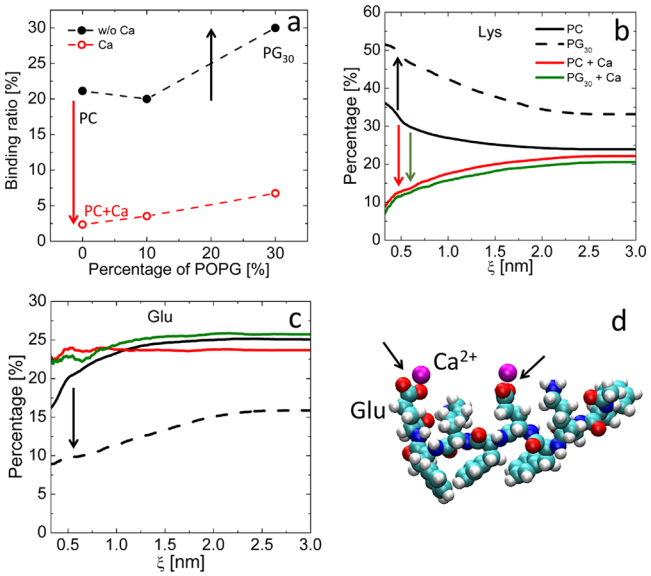

Figure 4. Binding of peptides to anionic bilayers. (a) Percentage of time that the F-peptide peptide binds to PC, PG_{10}, and PG_{30} bilayers. Arrows highlight effects of anionic lipid (in black) and Ca^{2+} ions (in red). Percentage of frames in our simulations for which (b) lysine and (c) glutamic acid are closer to the membrane than other residues at a distance ξ. Changes with respect to our reference simulation (PC bilayer) are shown with arrows. (d) Characteristic configuration showing Ca^{2+} ions bound to glutamic acid.

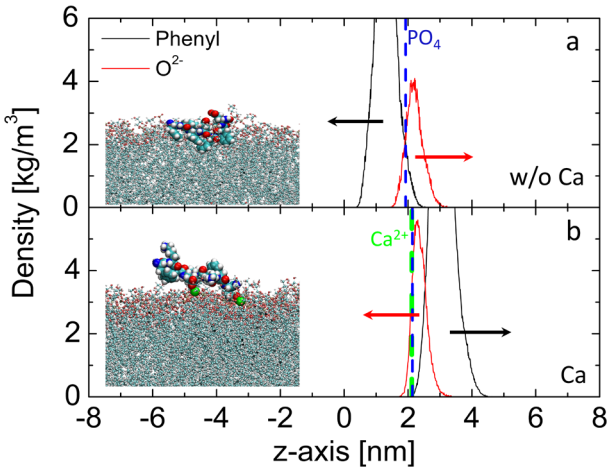

Figure 5. Density distributions of phenylalanine (black) and glutamic acid (red) in (a) the absence of $CaCl_2$ and (b) the presence of $CaCl_2$ for configuration in which the peptide is bound strongly to the bilayer. Characteristic configurations are shown in the inset with calcium ions being represented in green.

The addition of $CaCl_2$ to the solution accounts for a strong reduction (by almost 20%) in the percentage of bound states for both zwitterionic and anionic membranes, see Figure 4a. Panel b of this figure shows that the percentage of frames in which positively charged K residues are closest to the membrane decreases as ξ decreases for both zwitterionic PC (red lines) and anionic PG_{30} (green lines) bilayers. This implies that, in the presence of Ca^{2+} ions, K residues are repelled from the membrane. This is due to the deposition of Ca^{2+} ions on the bilayer (see Figure 2h), which accounts for a membrane surface that has a net positive charge. In our simulations, net charges of PC and PG_{30} bilayers due to the deposition of calcium ions are 29e and 13e, respectively. Surprisingly, panel c shows that, in the presence of Ca^{2+} ions, the percentage of frames in which negatively charged E residues are closer to the membrane than other residues is not strongly affected by the distance ξ for both zwitterionic PC (red line) and anionic PG_{30} (green line) membranes. This can be explained by the binding of Ca^{2+} ions to negatively charged E residues in the solution, see Figure 4d. This screens the electrostatic interaction between E residues and the positively charged membrane.

Strong Peptide–Membrane Binding. In the absence of Ca^{2+} ions, the peptide binds the membrane strongly in three and four of the five simulations performed using zwitterionic (i.e., PC) and anionic (i.e., PG_{30}) bilayers, respectively. Strong binding for these systems is characterized by the burial of nonpolar side chains of the peptide within the hydrophobic tails of lipids, while charged residues remain partially exposed to the solvent. To characterize this scenario, Figure 5a depicts density distributions of nonpolar F (in black) and negatively charged E (in red) side chains computed for configurations where the peptide is bound strongly to the membrane. Using the maximum in the density distribution of phosphate atoms as our reference (blue dashed line), this figure shows that F and E residues are located within the lipid tail and exposed to the solvent, respectively. A representative configuration depicting strong binding is shown in the inset of Figure 5a.

In the presence of Ca^{2+} ions, the peptide did not bind strongly in any of the simulations performed using PC or PG_{10} bilayers. However, strong binding was observed in one of the five simulations performed using PG_{30} bilayers. We also performed simulations in bilayers made from 100% POPG lipids in the presence of Ca^{2+} ions (results shown in Figure S2.4), and strong binding was observed in all five simulations. This type of strong binding in the presence of calcium is characterized by the formation of two Ca^{2+} bridges between E residues and phosphate moieties of lipid head groups. Density distributions of F (in black) and E (in red) side chains are shown in Figure 5b. In this figure, we also show positions of maximum densities of calcium ions (in dashed green) and phosphate atoms (in dashed blue). These positions coincide indicating strong binding between these species. Moreover, the distribution of E residues overlaps partially with distributions of both calcium ions and phosphate atoms suggesting Ca^{2+} bridges. The inset of Figure 5b provides an example of strong binding configuration in the presence of ions.

A Ca^{2+} bridge between negatively charged E residues and phosphate atoms was also reported in simulations performed using the Aβ protein.[45] In our simulations, calcium decreased significantly the peptide–membrane binding affinity (see Figure 4a), which is consistent with studies suggesting that Ca^{2+} ions prevent the insertion of peptides into the bilayer.[40] Importantly, in configurations where the peptide is bound strongly to the membrane via a Ca^{2+} bridge, F side chains are exposed to the solvent, see Figure 5b. We speculate that these exposed patches of non-polar residues could behave as hot spots for attracting peptides and catalyzing aggregation.

CONCLUSIONS

In summary, we performed extensive all-atom molecular dynamics simulations to study the interaction of amphipathic peptides with phospholipid bilayers. We show that both electrostatic and hydrophobic interactions contribute to

https://doi.org/10.1021/acschemneuro.1c00140
ACS Chem. Neurosci. 2021, 12, 2027–2035

binding. Specifically, positively charged residues are attracted to negatively charged phosphate moieties of lipid head groups. When the peptide is close to the membrane, hydrophobicity drives the burial of nonpolar residues into the bilayer. This produces strong binding of peptides to the bilayer. These mechanisms take place for both zwitterionic and anionic bilayers. For the latter membrane, the electrostatic attraction of positively charged residues is more pronounced than for the zwitterionic membrane. Accordingly, we observe stronger peptide-bilayer binding for anionic membranes compared to zwitterionic ones. We also show that Ca^{2+} ions are attracted to phosphate moieties of lipid head groups leaving the membrane with a net positive charge. This inhibits attraction of positive residues to the bilayer, accounting for a population of peptide−bilayer bound states that is significantly less pronounced than in our simulations containing $CaCl_2$ than in pure water. Strong binding of peptides to bilayers is also observed in simulations containing calcium, but it occurs less frequently than in simulations without calcium. It is driven by a Ca^{2+} bridge between negatively charged residues and phosphate moieties of lipids.

Mechanisms of interaction of antimicrobial peptides with lipid bilayers resemble those of amyloid peptides.[57] A vast majority of these peptides are cationic, and some of them form α-helices when their positive residues bind phosphate moieties of lipid head groups. This leaves the nonpolar side of the α-helix exposed to the solvent. Insertion of peptides into the membrane requires flipping the helix to enable hydrophobic residues to face the bilayer.[58] This membrane binding mechanism for antimicrobial peptides is very similar to the one outlined in this work for amyloid-like peptides. In particular, both mechanisms involve electrostatic attraction of peptides to the membrane surface followed by the insertion of nonpolar residues into the bilayer. This suggests that general principles govern the interaction of peptides with lipid bilayers independently of amino acid sequence.

Effects of cations are critical to understand interactions of peptides with lipid bilayers in amyloid diseases. In particular, it has been reported that concentrations of Ca^{2+} are dysregulated in cells overexpressing amyloids,[59] which is expected to affect the type and magnitude of membrane damage.[19] Our simulations show that Ca^{2+} ions reduce significantly the attraction of peptides to the bilayer. This is consistent with experimental studies, which have reported that calcium induces a shallower insertion of amyloid peptides into the bilayer causing less disruption of the membrane's hydrophobic core.[10,19,39] The main explanation of this phenomena in our simulations is the deposition of calcium into zwitterionic and anionic bilayers,[53,54] which shields the attraction of positively charged residues to negatively charged phosphate moieties of lipids. This general electrostatic principle is, therefore, likely to affect the interaction of other peptide−membrane systems. Accordingly, membrane permeabilization by some antimicrobial peptides, including alamethicin[60] and gramicidin,[61] is inhibited by calcium. Similarly, a recent study has shown that the attraction of actin filaments (which are negatively charged) to positively but not negatively charged membranes is reversed when divalent ions (i.e., Mg^{2+}) are added to the solutions.[62] Furthermore, experimental studies consistently show that calcium favors Aβ aggregation in the presence of vesicles.[19,39] Whereas our study does not address aggregation, we speculate that this effect of calcium can be explained by the reduced penetration of peptides into the bilayer where, surrounded by lipids, they cannot interact with other peptides easily. However, further simulations are needed to confirm this proposed role of Ca^{2+} in aggregation. Notice that, in addition to calcium, free lipids in solution may an also affect aggregation and the type of membrane damage caused by amyloids.[63]

METHODS

Two peptide sequences with alternating nonpolar and charged residues were studied, Ac-(**F**K**F**E)$_2$-NH_2 and Ac-(**V**K**V**E)$_2$-NH_2, see Figure 1a.[64,65] These amphipathic peptides differ in the nature of their nonpolar residues with the sequence containing phenylalanine (**F**) being more hydrophobic than the one with valine (**V**). These sequences are neutral as the number of positively charged lysine (K) and negatively charged glutamic acid (E) residues are the same. Experimental studies have shown that these peptides self-assembly forming cross-β structures that resemble amyloid fibrils.[64,65] CHARMM-GUI was used to build four different lipid bilayers[66−68] wherein our reference bilayer is made of 64 zwitterionic phosphatidylcholine (POPC) lipids in each leaflet. Three negatively charged membranes were studied by replacing POPC with 1-palmitoyl-2-oleoyl-*sn*-glycero-3-phospho-(1′-rac-glycerol) (POPG) to account for bilayers with 10%, 30%, and 100% anionic lipids. These bilayers will be referred to as PC, PG_{10}, PG_{30}, and PG. Atomic structures and charges of POPC and POPG are shown in Figure 1b. To neutralize the charge of the anionic bilayer, sodium ions are added to the solution as this ion does not bind strongly to lipids or peptide atoms.[53,54] To study the effect of Ca^{2+} on peptide−bilayer binding, simulations were performed in the presence and absence of $CaCl_2$ in the solution at an approximate concentration of 350 mM. Notice that the concentration of calcium in the extracellular space is on the order of 1−2 mM, which accounts for the presence of less than one calcium ion in a typical simulation box of size $7 \times 7 \times 7$ nm^3. Thus, following common practice in molecular dynamics simulations, we used a much higher concentration of calcium.[53,54] A summary of the different simulations performed in this work is provided in Table S1. Notice that five simulations were performed for each lipid composition and solvent condition. All the quantities reported in this work were computed from these five simulations.

Simulations were performed using GROMACS-2018[69] with the CHARMM36m force field and the TIP3P water model.[70] To model $CaCl_2$, we used the standard CHARMM36m force field as well as the NBFIX correction. The leapfrog algorithm was used to integrate the equations of motion with a 2 fs time step. Simulations were conducted in the NPT ensemble using the Nóse−Hoover thermostat (310 K and τ_T = 1 ps)[71,72] and the semi-isotropic Parrinello−Rahman barostat (1 bar and τ_P = 5 ps).[73] A Verlet-list was used to account for first-neighbors, and the cutoff for van der Waals interactions was set at 1.2 nm. Electrostatic interactions were treated using the Smooth Particle Mesh Ewald scheme with a grid spacing of 0.12 nm and a 1.2 nm real-space cutoff.[74]

ASSOCIATED CONTENT

Supporting Information

The Supporting Information is available free of charge at https://pubs.acs.org/doi/10.1021/acschemneuro.1c00140.

All the simulation setups, minimal distance between peptide and bilayer for systems studied, and the test of different force fields for calcium (PDF)

AUTHOR INFORMATION

Corresponding Author

Cristiano L. Dias − *Department of Physics, New Jersey Institute of Technology, Newark, New Jersey 07102-1982, United States;* orcid.org/0000-0002-8765-3922; Email: cld@njit.edu

https://doi.org/10.1021/acschemneuro.1c00140
ACS Chem. Neurosci. 2021, 12, 2027−2035

Authors

Yanxing Yang − *Department of Physics, New Jersey Institute of Technology, Newark, New Jersey 07102-1982, United States;* orcid.org/0000-0003-2521-6441

Sharareh Jalali − *Department of Physics, New Jersey Institute of Technology, Newark, New Jersey 07102-1982, United States*

Bradley L. Nilsson − *Department of Chemistry, University of Rochester, Rochester, New York 14627, United States;* orcid.org/0000-0003-1193-3693

Complete contact information is available at: https://pubs.acs.org/10.1021/acschemneuro.1c00140

Author Contributions

Y.Y. and C.L.D. designed the experiments. Y.Y. executed the simulations and performed analysis. S.J. assisted with the analysis. Y.Y., C.L.D., and B.L.N wrote the paper.

Notes

The authors declare no competing financial interest.

■ ACKNOWLEDGMENTS

This material is based upon the work supported by the National Science Foundation under Grant Nos. CHE-1904364 and CHE-1904528. Computational resources were provided by the High Performance Computing Center at NJIT and the Extreme Science and Engineering Discovery Environment (XSEDE) through allocation MCB-200049, which is supported by National Science Foundation grant number ACI-1548562.

■ REFERENCES

(1) Chiti, F., and Dobson, C. M. (2006) Protein misfolding, functional amyloid, and human disease. *Annu. Rev. Biochem. 75*, 333−366.

(2) Owen, M. C., Gnutt, D., Gao, M., Wärmländer, S. K., Jarvet, J., Gräslund, A., Winter, R., Ebbinghaus, S., and Strodel, B. (2019) Effects of in vivo conditions on amyloid aggregation. *Chem. Soc. Rev. 48*, 3946−3996.

(3) Hardy, J., and Allsop, D. (1991) Amyloid deposition as the central event in the aetiology of Alzheimer's disease. *Trends Pharmacol. Sci. 12*, 383−388.

(4) Hayden, E. Y., and Teplow, D. B. (2013) Amyloid β-protein oligomers and Alzheimer's disease. *Alzheimer's Res. Ther. 5*, 60.

(5) Benilova, I., Karran, E., and De Strooper, B. (2012) The toxic A-β oligomer and Alzheimer's disease: an emperor in need of clothes. *Nat. Neurosci. 15*, 349−357.

(6) Ow, S.-Y., and Dunstan, D. E. (2014) A brief overview of amyloids and Alzheimer's disease. *Protein Sci. 23*, 1315−1331.

(7) Kayed, R. (2003) Common structure of soluble amyloid oligomers implies common mechanism of pathogenesis. *Science 300*, 486−489.

(8) Haass, C., and Selkoe, D. J. (2007) Soluble protein oligomers in neurodegeneration: lessons from the Alzheimer's amyloid β-peptide. *Nat. Rev. Mol. Cell Biol. 8*, 101−112.

(9) Chimon, S., Shaibat, M. A., Jones, C. R., Calero, D. C., Aizezi, B., and Ishii, Y. (2007) Evidence of fibril-like β-sheet structures in a neurotoxic amyloid intermediate of Alzheimer's β-amyloid. *Nat. Struct. Mol. Biol. 14*, 1157−1164.

(10) Sciacca, M. F., Kotler, S. A., Brender, J. R., Chen, J., Lee, D.-k., and Ramamoorthy, A. (2012) Two-step mechanism of membrane disruption by A-β through membrane fragmentation and pore formation. *Biophys. J. 103*, 702−710.

(11) Stefani, M., and Dobson, C. M. (2003) Protein aggregation and aggregate toxicity: new insights into protein folding, misfolding diseases and biological evolution. *J. Mol. Med. 81*, 678−699.

(12) Bezprozvanny, I., and Mattson, M. P. (2008) Neuronal calcium mishandling and the pathogenesis of Alzheimer's disease. *Trends Neurosci. 31*, 454−463.

(13) Cecchi, C., Baglioni, S., Fiorillo, C., Pensalfini, A., Liguri, G., Nosi, D., Rigacci, S., Bucciantini, M., and Stefani, M. (2005) Insights into the molecular basis of the differing susceptibility of varying cell types to the toxicity of amyloid aggregates. *J. Cell Sci. 118*, 3459−3470.

(14) Habchi, J., Chia, S., Galvagnion, C., Michaels, T. C. T., Bellaiche, M. M. J., Ruggeri, F. S., Sanguanini, M., Idini, I., Kumita, J. R., Sparr, E., et al. (2018) Cholesterol catalyses Aβ42 aggregation through a heterogeneous nucleation pathway in the presence of lipid membranes. *Nat. Chem. 10*, 673−683.

(15) Zhang, X., St. Clair, J. R., London, E., and Raleigh, D. P. (2017) Islet amyloid polypeptide membrane interactions: effects of membrane composition. *Biochemistry 56*, 376−390.

(16) Straub, J. E., and Thirumalai, D. (2014) Membrane−protein interactions are key to understanding amyloid formation. *J. Phys. Chem. Lett. 5*, 633−635.

(17) Drolle, E., Negoda, A., Hammond, K., Pavlov, E., and Leonenko, Z. (2017) Changes in lipid membranes may trigger amyloid toxicity in Alzheimer's disease. *PLoS One 12*, No. e0182194.

(18) Bucciantini, M., Rigacci, S., and Stefani, M. (2014) Amyloid aggregation: Role of biological membranes and the aggregate−membrane system. *J. Phys. Chem. Lett. 5*, 517−527.

(19) Sciacca, M. F. M., Monaco, I., La Rosa, C., and Milardi, D. (2018) The active role of Ca^{2+} ions in Aβ-mediated membrane damage. *Chem. Commun. 54*, 3629−3631.

(20) Liu, Y., Ren, B., Zhang, Y., Sun, Y., Chang, Y., Liang, G., Xu, L., and Zheng, J. (2018) Molecular simulation aspects of amyloid peptides at membrane interface. *Biochim. Biophys. Acta, Biomembr. 1860*, 1906−1916.

(21) Dias, C. L., Jalali, S., Yang, Y., and Cruz, L. (2020) Role of Cholesterol on Binding of Amyloid Fibrils to Lipid Bilayers. *J. Phys. Chem. B 124*, 3036.

(22) Hane, F., Drolle, E., Gaikwad, R., Faught, E., and Leonenko, Z. (2011) Amyloid-beta aggregation on model lipid membranes: an atomic force microscopy study. *J. Alzheimer's Dis. 26*, 485−494.

(23) Drolle, E., Gaikwad, R. M., and Leonenko, Z. (2012) Nanoscale electrostatic domains in cholesterol-laden lipid membranes create a target for amyloid binding. *Biophys. J. 103*, L27−L29.

(24) Manna, M., and Mukhopadhyay, C. (2013) Binding, conformational transition and dimerization of amyloid-beta peptide on GM1-containing ternary membrane: insights from molecular dynamics simulation. *PLoS One 8*, No. e71308.

(25) Ntarakas, N., Ermilova, I., and Lyubartsev, A. P. (2019) Effect of lipid saturation on amyloid-beta peptide partitioning and aggregation in neuronal membranes: molecular dynamics simulations. *Eur. Biophys. J. 48*, 813−824.

(26) Kinnunen, P. K. (2010) Amyloid formation on lipid membrane surfaces. *Open Biol. J. 2*, 163−175.

(27) Tipping, K. W., Karamanos, T. K., Jakhria, T., Iadanza, M. G., Goodchild, S. C., Tuma, R., Ranson, N. A., Hewitt, E. W., and Radford, S. E. (2015) pH-induced molecular shedding drives the formation of amyloid fibril-derived oligomers. *Proc. Natl. Acad. Sci. U. S. A. 112*, 5691−5696.

(28) Hellstrand, E., Sparr, E., and Linse, S. (2010) Retardation of Abeta fibril formation by phospholipid vesicles depends on membrane phase behavior. *Biophys. J. 98*, 2206−2214.

(29) Bonev, B., Watts, A., Bokvist, M., and Gröbner, G. (2001) Electrostatic peptide−lipid interactions of amyloid-beta peptide and pentalysine with membrane surfaces monitored by 31P MAS NMR. *Phys. Chem. Chem. Phys. 3*, 2904−2910.

(30) Moores, B., Drolle, E., Attwood, S. J., Simons, J., and Leonenko, Z. (2011) Effect of surfaces on amyloid fibril formation. *PLoS One 6*, No. e25954.

(31) Lindberg, D. J., Wesén, E., Björkeroth, J., Rocha, S., and Esbjörner, E. K. (2017) Lipid membranes catalyse the fibril formation of the amyloid-β (1−42) peptide through lipid-fibril interactions that

reinforce secondary pathways. *Biochim. Biophys. Acta, Biomembr. 1859*, 1921−1929.
(32) Lee, H.-J., Choi, C., and Lee, S.-J. (2002) Membrane-bound α-synuclein has a high aggregation propensity and the ability to seed the aggregation of the cytosolic form. *J. Biol. Chem. 277*, 671−678.
(33) Sparr, E., Engel, M. F., Sakharov, D. V., Sprong, M., Jacobs, J., de Kruijff, B., Höppener, J. W., and Antoinette Killian, J. (2004) Islet amyloid polypeptide-induced membrane leakage involves uptake of lipids by forming amyloid fibers. *FEBS Lett. 577*, 117−120.
(34) Zhu, M., Souillac, P. O., Ionescu-Zanetti, C., Carter, S. A., and Fink, A. L. (2002) Surface-catalyzed amyloid fibril formation. *J. Biol. Chem. 277*, 50914−50922.
(35) Ji, S.-R., Wu, Y., and Sui, S.-f. (2002) Cholesterol is an important factor affecting the membrane insertion of β-amyloid peptide (Aβ1−40), which may potentially inhibit the fibril formation. *J. Biol. Chem. 277*, 6273−6279.
(36) Chi, E. Y., Ege, C., Winans, A., Majewski, J., Wu, G., Kjaer, K., and Lee, K. Y. C. (2008) Lipid membrane templates the ordering and induces the fibrillogenesis of Alzheimer's disease amyloid-β peptide. *Proteins: Struct., Funct., Genet. 72*, 1−24.
(37) Chauhan, A., Ray, I., and Chauhan, V. P. (2000) Interaction of amyloid beta-protein with anionic phospholipids: possible involvement of Lys28 and C-terminus aliphatic amino acids. *Neurochem. Res. 25*, 423−429.
(38) Kang, C., and Sun, R. (2021) Molecular dynamics study of the interaction between the N-terminal of alpha-synuclein and a lipid bilayer mimicking synaptic vesicles. *J. Phys. Chem. B 125*, 1036−1048.
(39) Sciacca, M. F., Milardi, D., Messina, G. M., Marletta, G., Brender, J. R., Ramamoorthy, A., and La Rosa, C. (2013) Cations as switches of amyloid-mediated membrane disruption mechanisms: calcium and IAPP. *Biophys. J. 104*, 173−184.
(40) Meratan, A. A., Ghasemi, A., and Nemat-Gorgani, M. (2011) Membrane integrity and amyloid cytotoxicity: a model study involving mitochondria and lysozyme fibrillation products. *J. Mol. Biol. 409*, 826−838.
(41) Ohnishi, S., and Ito, T. (1974) Calcium-induced phase separations in phosphatidylserine-phosphatidylcholine membranes. *Biochemistry 13*, 881−887.
(42) Tamamizu-Kato, S., Kosaraju, M. G., Kato, H., Raussens, V., Ruysschaert, J.-M., and Narayanaswami, V. (2006) Calcium-triggered membrane interaction of the α-synuclein acidic tail. *Biochemistry 45*, 10947−10956.
(43) Gerke, V., Creutz, C. E., and Moss, S. E. (2005) Annexins: linking Ca^{2+} signalling to membrane dynamics. *Nat. Rev. Mol. Cell Biol. 6*, 449−461.
(44) Lockhart, C., and Klimov, D. K. (2015) Calcium enhances binding of Aβ monomer to DMPC lipid bilayer. *Biophys. J. 108*, 1807−1818.
(45) Yi, X., Zhang, Y., Gong, M., Yu, X., Darabedian, N., Zheng, J., and Zhou, F. (2015) Ca^{2+} interacts with Glu-22 of Aβ (1−42) and phospholipid bilayers to accelerate the Aβ (1−42) aggregation below the critical micelle concentration. *Biochemistry 54*, 6323−6332.
(46) Lemkul, J. A., and Bevan, D. R. (2009) Perturbation of membranes by the amyloid beta-peptide - a molecular dynamics study. *FEBS J. 276*, 3060−3075.
(47) Brown, A. M., and Bevan, D. R. (2016) Molecular dynamics simulations of amyloid beta-peptide (1−42): tetramer formation and membrane interactions. *Biophys. J. 111*, 937−949.
(48) Yu, X., Wang, Q., Pan, Q., Zhou, F., and Zheng, J. (2013) Molecular interactions of Alzheimer amyloid-β oligomers with neutral and negatively charged lipid bilayers. *Phys. Chem. Chem. Phys. 15*, 8878.
(49) Jang, H., Zheng, J., and Nussinov, R. (2007) Models of beta-amyloid ion channels in the membrane suggest that channel formation in the bilayer is a dynamic process. *Biophys. J. 93*, 1938−1949.
(50) Friedman, R., Pellarin, R., and Caflisch, A. (2009) Amyloid aggregation on lipid bilayers and its impact on membrane permeability. *J. Mol. Biol. 387*, 407−415.
(51) Lockhart, C., Smith, A. K., and Klimov, D. K. (2020) Three popular force fields predict consensus mechanism of amyloid β peptide binding to the dimyristoylgylcerophosphocholine bilayer. *J. Chem. Inf. Model. 60*, 2282−2293.
(52) Lockhart, C., and Klimov, D. K. (2014) Alzheimer's Aβ10−40 peptide binds and penetrates DMPC bilayer: an isobaric−isothermal replica exchange molecular dynamics study. *J. Phys. Chem. B 118*, 2638−2648.
(53) Javanainen, M., Melcrová, A., Magarkar, A., Jurkiewicz, P., Hof, M., Jungwirth, P., and Martinez-Seara, H. (2017) Two cations, two mechanisms: interactions of sodium and calcium with zwitterionic lipid membranes. *Chem. Commun. 53*, 5380−5383.
(54) Catte, A., Girych, M., Javanainen, M., Loison, C., Melcr, J., Miettinen, M. S., Monticelli, L., Määttä, J., Oganesyan, V. S., Ollila, O. H. S., et al. (2016) Molecular electrometer and binding of cations to phospholipid bilayers. *Phys. Chem. Chem. Phys. 18*, 32560−32569.
(55) Kohagen, M., Mason, P. E., and Jungwirth, P. (2014) Accurate description of calcium solvation in concentrated aqueous solutions. *J. Phys. Chem. B 118*, 7902−7909.
(56) Han, K., Venable, R. M., Bryant, A.-M., Legacy, C. J., Shen, R., Li, H., Roux, B., Gericke, A., and Pastor, R. W. (2018) Graph−theoretic analysis of monomethyl phosphate clustering in ionic solutions. *J. Phys. Chem. B 122*, 1484−1494.
(57) Ernst, C. M., and Peschel, A. (2011) Broad-spectrum antimicrobial peptide resistance by MprF-mediated aminoacylation and flipping of phospholipids. *Mol. Microbiol. 80*, 290−299.
(58) Park, P., Franco, L. R., Chaimovich, H., Coutinho, K., Cuccovia, I. M., and Lima, F. S. (2019) Binding and flip as initial steps for BP-100 antimicrobial actions. *Sci. Rep. 9*, 8622.
(59) Parkash, J., Chaudhry, M. A., Amer, A. S., Christakos, S., and Rhoten, W. B. (2002) Intracellular Calcium Ion Response to Glucose in β-Cells of Calbindin-D_{28k} Nullmutant Mice and in βHC13 Cells Overexpressing Calbindin-D_{28k}. *Endocr. J. 18*, 221−230.
(60) Hall, J. E., and Cahalan, M. D. (1982) Calcium-induced inactivation of alamethicin in asymmetric lipid bilayers. *J. Gen. Physiol. 79*, 387−409.
(61) Gambale, F., Menini, A., and Rauch, G. (1987) Effects of calcium on the gramicidin A single channel in phosphatidylserine membranes. *Eur. Biophys. J. 14*, 369−374.
(62) Schroer, C., Baldauf, L., van Buren, L., Wassenaar, T., Melo, M., Koenderink, G., and Marrink, S. (2020) Charge-dependent interactions of monomeric and filamentous actin with lipid bilayers. *Proc. Natl. Acad. Sci. U. S. A. 117*, 5861−5872.
(63) Sciacca, M. F., Lolicato, F., Tempra, C., Scollo, F., Sahoo, B. R., Watson, M. D., García-Viñuales, S., Milardi, D., Raudino, A., Lee, J. C., Ramamoorthy, A., and La Rosa, C. (2020) Lipid-chaperone hypothesis: a common molecular mechanism of membrane disruption by intrinsically disordered proteins. *ACS Chem. Neurosci. 11*, 4336−4350.
(64) Bowerman, C. J., and Nilsson, B. L. (2010) A reductive trigger for peptide self-assembly and hydrogelation. *J. Am. Chem. Soc. 132*, 9526−9527.
(65) Marini, D. M., Hwang, W., Lauffenburger, D. A., Zhang, S., and Kamm, R. D. (2002) Left-handed helical ribbon intermediates in the self-assembly of a β-sheet peptide. *Nano Lett. 2*, 295−299.
(66) Lee, J., Cheng, X., Swails, J. M., Yeom, M. S., Eastman, P. K., Lemkul, J. A., Wei, S., Buckner, J., Jeong, J. C., Qi, Y., et al. (2016) CHARMM-GUI input generator for NAMD, GROMACS, AMBER, OpenMM, and CHARMM/OpenMM simulations using the CHARMM36 additive force field. *J. Chem. Theory Comput. 12*, 405−413.
(67) Jo, S., Lim, J. B., Klauda, J. B., and Im, W. (2009) CHARMM-GUI membrane builder for mixed bilayers and its application to yeast membranes. *Biophys. J. 97*, 50−58.
(68) Jo, S., Kim, T., Iyer, V. G., and Im, W. (2008) CHARMM-GUI: a web-based graphical user interface for CHARMM. *J. Comput. Chem. 29*, 1859−1865.
(69) Abraham, M. J., Murtola, T., Schulz, R., Páll, S., Smith, J. C., Hess, B., and Lindahl, E. (2015) GROMACS: High performance

https://doi.org/10.1021/acschemneuro.1c00140
ACS Chem. Neurosci. 2021, 12, 2027−2035

molecular simulations through multi-level parallelism from laptops to supercomputers. *SoftwareX 1*, 19−25.
(70) Klauda, J. B., Venable, R. M., Freites, J. A., O'Connor, J. W., Tobias, D. J., Mondragon-Ramirez, C., Vorobyov, I., MacKerell, A. D., and Pastor, R. W. (2010) Update of the CHARMM all-atom additive force field for lipids: validation on six lipid types. *J. Phys. Chem. B 114*, 7830−7843.
(71) Nosé, S. (1984) A unified formulation of the constant temperature molecular dynamics methods. *J. Chem. Phys. 81*, 511−519.
(72) Hoover, W. G. (1985) Canonical dynamics: equilibrium phase-space distributions. *Phys. Rev. A: At., Mol., Opt. Phys. 31*, 1695−1697.
(73) Parrinello, M., and Rahman, A. (1981) Polymorphic transitions in single crystals: a new molecular dynamics method. *J. Appl. Phys. 52*, 7182−7190.
(74) Darden, T., York, D., and Pedersen, L. (1993) Particle mesh Ewald: an Nlog(N) method for Ewald sums in large systems. *J. Chem. Phys. 98*, 10089−10092.

https://doi.org/10.1021/acschemneuro.1c00140
ACS Chem. Neurosci. 2021, 12, 2027−2035